

**VICTORIA UNIVERSITY**  
MELBOURNE AUSTRALIA

*Intrinsically modified self-extinguishing fire-retardant epoxy resin using boron-polyol complex*

This is the Published version of the following publication

Mathews, Lalson Daniel, Capricho, Jaworski C, Salim, Nisa, Parameswaranpillai, Jyotishkumar, Moinuddin, Khalid and Hameed, Nishar (2023) Intrinsically modified self-extinguishing fire-retardant epoxy resin using boron-polyol complex. *Journal of Polymer Research*, 30 (7). ISSN 1022-9760

The publisher's official version can be found at  
<https://link.springer.com/article/10.1007/s10965-023-03641-6>  
Note that access to this version may require subscription.

Downloaded from VU Research Repository <https://vuir.vu.edu.au/47964/>



# Intrinsically modified self-extinguishing fire-retardant epoxy resin using boron-polyol complex

Lalson Daniel Mathews<sup>1</sup> · Jaworski C. Capricho<sup>1</sup> · Nisa Salim<sup>1</sup> · Jyotishkumar Parameswaranpillai<sup>2</sup> · Khalid Moinuddin<sup>3</sup> · Nishar Hameed<sup>1</sup>

Received: 30 June 2022 / Accepted: 30 May 2023 / Published online: 22 June 2023  
© The Author(s) 2023

## Abstract

A novel fire-retardant epoxy thermoset, containing boron polyol complex, was prepared and characterised. The fire-retardant additive was a stoichiometric mixture of boric acid and glycerol. Flame retardancy of the epoxy resin was improved by the formation of stable char layer that protected the underlying epoxy from further burning. Phonon transport through the polymer matrix via hydrogen bonding was identified. The hydrogen bonding acted as a thermal bridge for intermolecular phonon transport to gain improved thermal conductivity resulting early char formation. The hydrogen bonding between the complex and the epoxy matrix was demonstrated using Fourier Transform Infrared Spectroscopy. The phonon transport and a high degree of graphitization was confirmed using Raman Spectroscopy. Thermogravimetric analysis was used for polymer decomposition to confirm a char yield of over 20%. Reaction to fire test revealed enhancement in fire retardancy and self-extinguishing properties of the blend compared to the neat epoxy. Cone calorimetry testing confirmed decreased peak heat release rate and total smoke production by the effect of boron compound in the epoxy matrix. Hydrogen bonding, formation of thick stable layer of char at the polymer surface, and a blowing out effect caused by pyrolytic gases escaping to the gaseous phase, were attributed to the improved fire retardancy. This research may find applications in thermal insulation material of electronic circuit boards, coating in aerospace materials, as well as building and construction industries.

**Keywords** Fire retardancy · Epoxy polymers · Boron complex · Hydrogen bonding · Thermal conductivity · Char formation · Fire hazard

## Introduction

Epoxy resins represent a large group of thermoset polymers with unique mechanical, electrical, and chemical properties. Epoxy composites and blends are popularly used in many industries such as aerospace, automotive, defence, electronics, and construction [1]. Being a product derived from petroleum, epoxy resins are inherently flammable, and may represent a fire hazard in high temperature environments.

Intrinsic modification of the epoxy resins, blending epoxy resins with fire retardants, and epoxy-composite fabrication are few important methods to improve fire retardancy. In particular, altering polymer properties in the molecular level has been an efficient technique for reducing flammability. In recent years, materials including benzoxazines, ammonium polyphosphate, 9,10-dihydro-9-oxa-10-phosphaphenanthrene-10-oxide, boron nitride nanosheets and bio-based materials such as vanillin, genistein, resveratrol have been successfully utilised for reducing flammability of epoxy resins [2–9].

A typical drawback of many fire-retardant additives is the negative impact when released into the environment. Most fire-resistant materials are not eco-friendly. The popular flame retardant additives on the market are halogenated ones [10] but unfortunately majority of them are harmful chemicals. The use of organohalogen flame retardants are controlled with strict regulations and its replacement products such as organophosphate ester flame retardants are under

✉ Nishar Hameed  
nisharhameed@swin.edu.au

<sup>1</sup> School of Engineering, Swinburne University of Technology, Hawthorn, VIC 3122, Australia

<sup>2</sup> Department of Science, Faculty of Science & Technology, Alliance University, Chandapura-Anekal Main Road, 562106 Bengaluru, India

<sup>3</sup> Institute of Sustainable Industries and Liveable Cities (ISILC), Victoria University, Werribee, VIC 3030, Australia



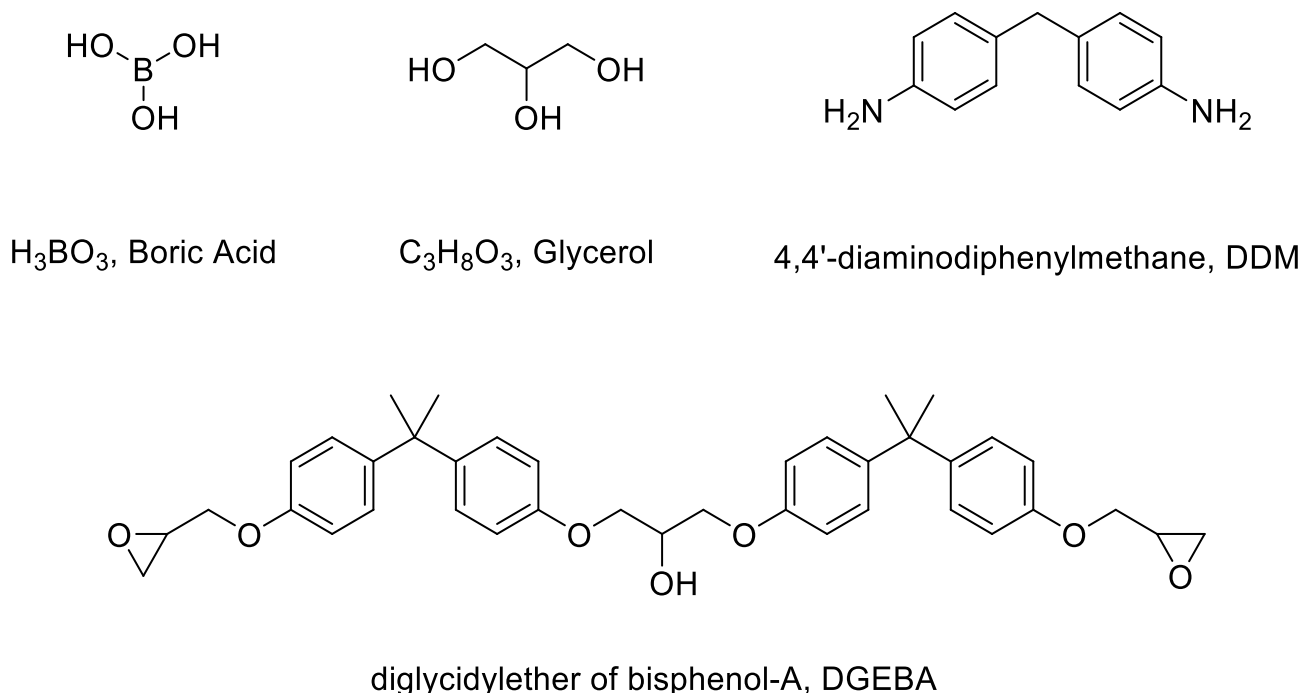


**Fig. 3** Chemical structure of materials used to synthesise fire retardant epoxy blend

Sigma-Aldrich. The chemical structures of these compounds are shown in Fig. 3.

### Synthesis of fire-retardant epoxy blend

The fire-retardant epoxy resin blend was synthesised in two steps. A 25% mixture of boric acid in glycerol (BPC) was prepared by mixing 17.5 g boric acid in 52.5 g glycerol at 40 °C under constant stirring in a conical flask until boric acid was completely dissolved. The resultant mixture was highly viscous, saturated with boric acid devoid of any neutralising agents [16]. Boric acid was completely dissolved in glycerol at 40 °C.

In the second step, the BPC complex was blended with DGEBA resin under constant stirring at 40 °C until homogenised, followed by the addition of proportionate amount of DDM. The mixture was thoroughly blended and degassed, allowed to settle under room temperature prior to curing at 120 °C for 24 h in an oven and post curing at 180 °C for 1 h. The mixing ratio and compositions were detailed in Table 1.

### Characterization

**Differential scanning calorimetry (DSC)** Phase behavior of the blend was investigated using a NETZSCH-PROTEUS-70 DSC. The cured polymer samples were heated

**Table 1** DGEBA-BPC composition

Polymer ID	Mixing ratio			Composition			
	DGEBA (g)	BPC Soln. (g)	Hardener (g)	PHR of BPC Soln.	Boric acid (g)	Boron equivalent (g)	% Boron in cured thermoset
DGEBA-0	5	0	1.5	0	0	0	0
DGEBA-0.5	5	0.5	1.5	10	0.125	0.022	0.31
DGEBA-1	5	1	1.5	20	0.25	0.044	0.58
DGEBA-2	5	2	1.5	40	0.5	0.088	1.03
DGEBA-3	5	3	1.5	60	0.75	0.132	1.39
DGEBA-4	5	4	1.5	80	1	0.175	1.67
DGEBA-5	5	5	1.5	100	1.25	0.219	1.91

up to 100 °C with temperature ramp rate of 20 °C/min and held for 5 min at 100 °C. Then the samples were cooled down to -30 °C and then reheated to 250 °C at 20 °C/min. The glass transition temperature ( $T_g$ ) was measured at the midpoint of transition.

**Thermogravimetric analysis (TGA)** The thermal stability and char formation of the cured epoxy blend was investigated using Q500 TGA instrument. Samples was heated in a platinum pan up to 800 °C with 10 °C per minute increment under N<sub>2</sub> environment.

**Fourier transform infrared (FTIR) spectroscopy** KBr method was used to determine the FTIR characteristics of the blend on a Bruker FTIR spectrometer. The cured solid samples were placed on the clean surface of sample holder. The spectra were recorded in the standard wavenumbers range of 400 and 4000 cm<sup>-1</sup> at an average 28 scans.

**Vertical burning test** The specimens were tested for vertical flammability under laboratory conditions at a wind speed of 0.2–0.4 m/s and an ambient temperature of 23 °C.

**Cone calorimetry** Cone calorimetry test was carried out using the iCone cone calorimeter with the heat flux of 50 kW/m<sup>2</sup> on a 100 mm × 100 mm carbon fiber (CF) reinforced epoxy composite system. The rough side of the specimen was the exposed face, and the unexposed face was covered with aluminium foil. The CF composites were prepared by hand layup method.

**Raman spectroscopy** Raman spectrum of the char layer and the unburned blend was captured by Renishaw inVia Raman instrument. A 514 nm laser wavelength was selected to analyse graphitization.

**Optical microscope** Structure of the char layer was analyzed under the optical digital microscope Olympus BX61.

## Result and discussion

### Fourier transform infrared spectroscopy

Infrared spectrum of the polymer exhibited significant changes in the hydroxyl group region of DGEBA-BPC polymer that can be explained in connection with the hydrogen bonding between BPC and DGEBA-DDM as illustrated in Fig. 4. Intermolecular hydrogen bonding in epoxy was beneficial for improved phonon transport through the matrix [28, 29], which in turn accelerated thermal conductivity [28] to promote char formation, that resulted in better flame retardancy. Hydrogen bonding enabled a thermal connection between DGEBA and BPC to form a strong linear network for phonon transport.

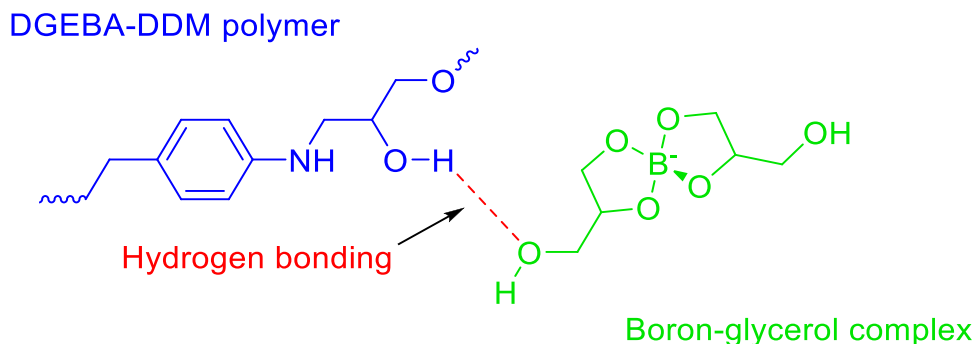
Initially, the structure of BPC was analysed using FTIR spectroscopy. Figure 5 represents FTIR spectral comparison of boric acid, glycerol, and BPC complex.

In boric acid spectrum, peaks at 548 and 710 cm<sup>-1</sup> linked to boric acid (H<sub>3</sub>BO<sub>3</sub>). Peak at 631 cm<sup>-1</sup> represented deformation vibrations of atoms in B-O [30]. Peak at 1194 cm<sup>-1</sup> belonged to -O-B < vibrations in orthoboric acid [31] that disappeared in BPC complex and did not exist in BPC as confirmed from previous report [32]. In glycerol spectrum, the C-H stretching vibrations at 2931 and 2875 cm<sup>-1</sup> were replicated in the BPC complex.

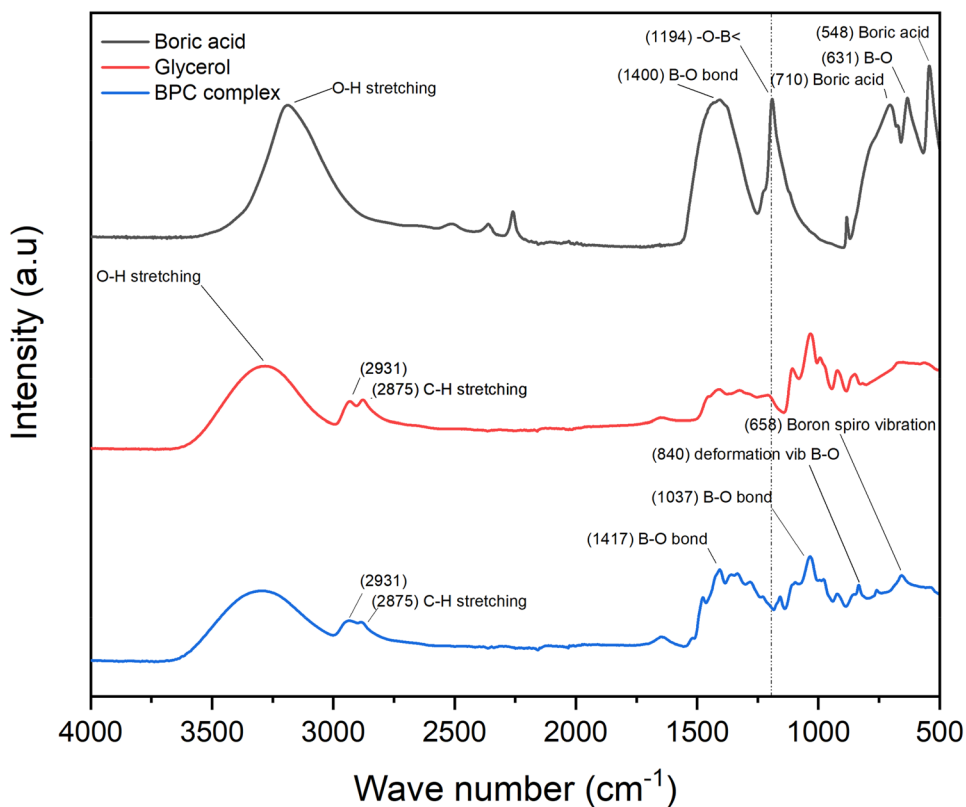
In the BPC complex spectrum, peaks at 1037 cm<sup>-1</sup> and 1417 cm<sup>-1</sup> were the symmetric and asymmetric stretching vibrations of B-O bond. Boron spiro structure vibration was observed at 658 cm<sup>-1</sup> and B-O deformation vibration at 840 cm<sup>-1</sup> [32].

Figure 6 represents the hydroxyl stretching region from 3100 cm<sup>-1</sup> to 3600 cm<sup>-1</sup> of neat and blend DGEBA in the infrared spectrum. Neat epoxy showed two important bands at 3390 and 3545 cm<sup>-1</sup>, attributed to self-associated hydroxyl groups and non-associated free hydroxyl groups respectively. The shoulder peak at 3545 cm<sup>-1</sup> - as seen in neat DGEBA - was the free hydroxyl groups which

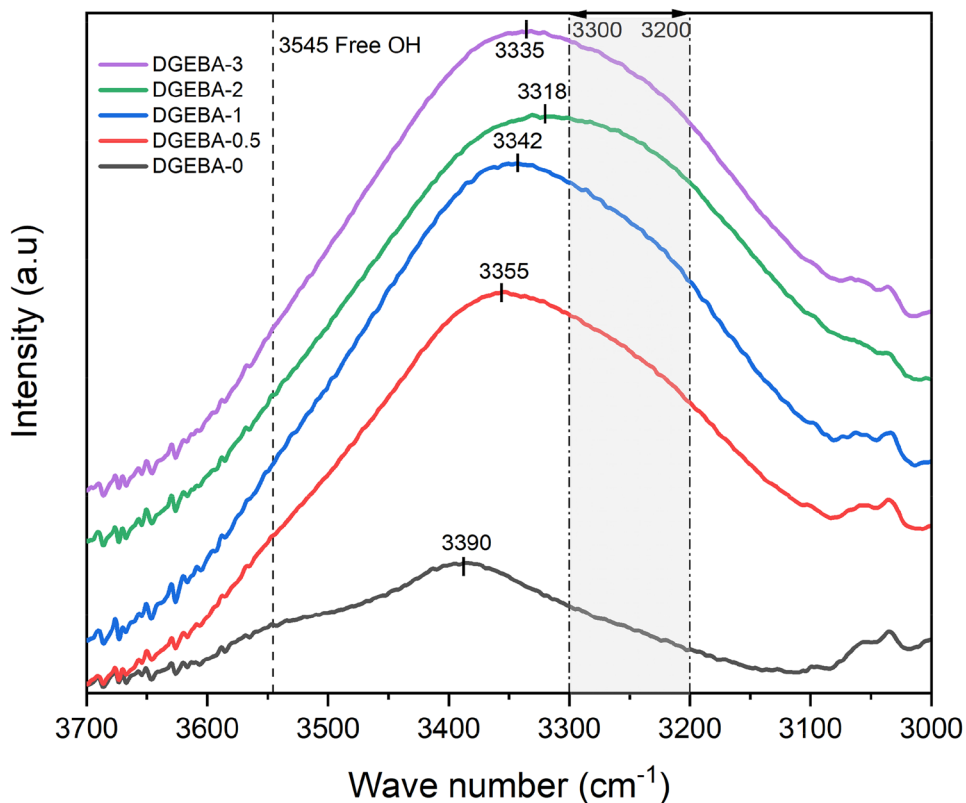
**Fig. 4** Hydrogen bonding between BPC and DGEBA-DDM at the hydroxyl groups



**Fig. 5** FTIR spectrum of Boric acid, glycerol, and BPC complex comparison



**Fig. 6** FTIR peaks confirming hydrogen bonding in DGEBA blend with BPC



disappeared with increased addition of BPC. This indicated that the free hydroxyl group of the DGEBA created a hydrogen bonding with hydroxyl group of BPC complex (Fig. 4) [33].

The peak at  $3390\text{ cm}^{-1}$  represented the stretching vibration of self-associated hydroxyl group in neat DGEBA, which shifted towards lower wave number region with the addition of BPC complex, confirming hydrogen bonding [34, 35] and increased bond length as a result. It has been proven in previous studies that a hydrogen bond could increase the bond length of C-O bond in an epoxide [36, 37] and a similar increase in bond length is observed in C-O bond linked to the hydroxyl group here. DGEBA contained an ether group (-O-) which is an acceptor, and a hydroxyl group (-OH) which is both an acceptor and a donor of hydrogen bonds with the hydroxyl group of BPC [38]. A hydrogen bond formed at the hydroxyl group of DGEBA contributed to the peak shift at  $3390\text{ cm}^{-1}$  (Fig. 6). This reconfirmed the formation of hydrogen bonding between free hydroxyl group and BPC.

In addition to that, the spectral region between  $3200$  and  $3300\text{ cm}^{-1}$  showed an increasing bulge that exhibited the presence of O-H bonds [39] originated from hydrogen bonding between the hydroxyl groups of cured DGEBA and BPC.

Figure 7 compared the FTIR spectrums of BPC complex, neat DGEBA and 20phr DGEBA-BPC blend. The bimodal peak around  $2900\text{ cm}^{-1}$  represented the C-H symmetric and asymmetric stretching vibrations. The corresponding peaks at  $2930\text{ cm}^{-1}$  and  $2880\text{ cm}^{-1}$  of glycerol was present in BPC complex [40] with higher intensity indicating increased amount of C-H bonds in the blend contributed from the BPC additive. In addition to that, a broadening of the hydroxyl group is attributed to the cross-linking reaction and formation of hydrogen bonds.

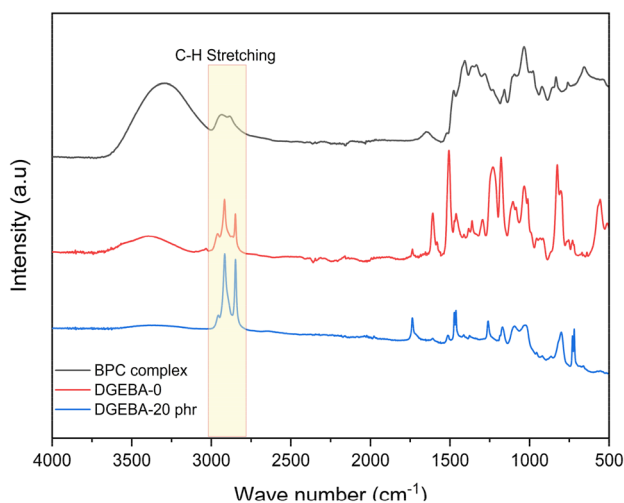


Fig. 7 FTIR spectrum of BPC complex, neat epoxy and 20 phr blend

## Differential scanning calorimetry

Transition from solid crystalline state to amorphous rubbery state was evaluated by DSC to characterise the physical properties and phase behaviour of the polymer blends (Fig. 8).

The steady decrease in  $T_g$  is attributed to the increased free volume of DGEBA with the addition of BPC.  $T_g$  of polymers is a factor of the mobility of polymer chain where an increased free volume in a polymer structure will reduce its  $T_g$  [41, 42]. Plasticization effect is a direct result of increased free volume. Low melting point of glycerol boosts the plasticization effect of DGEBA resulting in decreased  $T_g$ . Secondly,  $T_g$  of a polymer network is related to reactive hydrogen bonding [43]. Decrease in  $T_g$  is also explained by lower degree of solidification due to steric hindrance in the curing ring opening reaction to reduce the cross-linking density [44, 45].

## Thermogravimetric analysis

Figure 9 illustrated the thermal degradation diagrams of neat DGEBA and the blends. The results showed that neat DGEBA and blends had similar one-stage degradation. This is due to the decomposition of macromolecular chains of epoxy involving the degradation of C-O-C and C-C bonds from the epoxy resin [46]. Neat DGEBA lost 8% of its total weight at  $800\text{ }^\circ\text{C}$  whereas DGEBA-0.5 and DGEBA-1 lost only 7% and 7% respectively preserving 2% and 2% of their original weight. This implied the increased amount of char formation and presence of non-combustible materials. DGEBA-2 onwards showed a reverse trend in weight loss due to unreacted combustible BPC complex in epoxy matrix. First derivative of weight loss percentage against temperature curve (DTG) indicated increase in degradation temperature with the increased addition of BPC complex

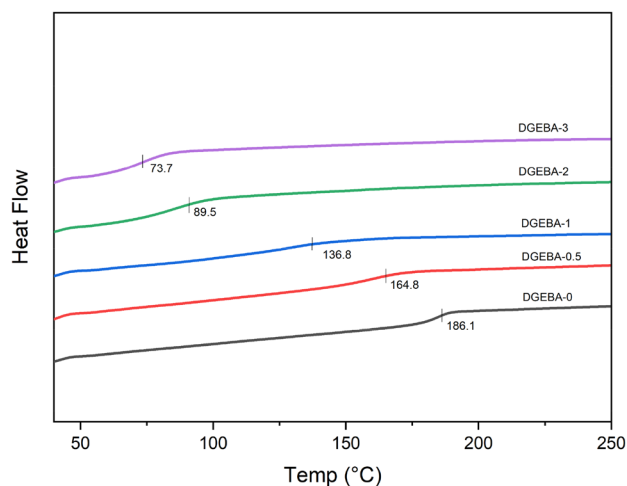
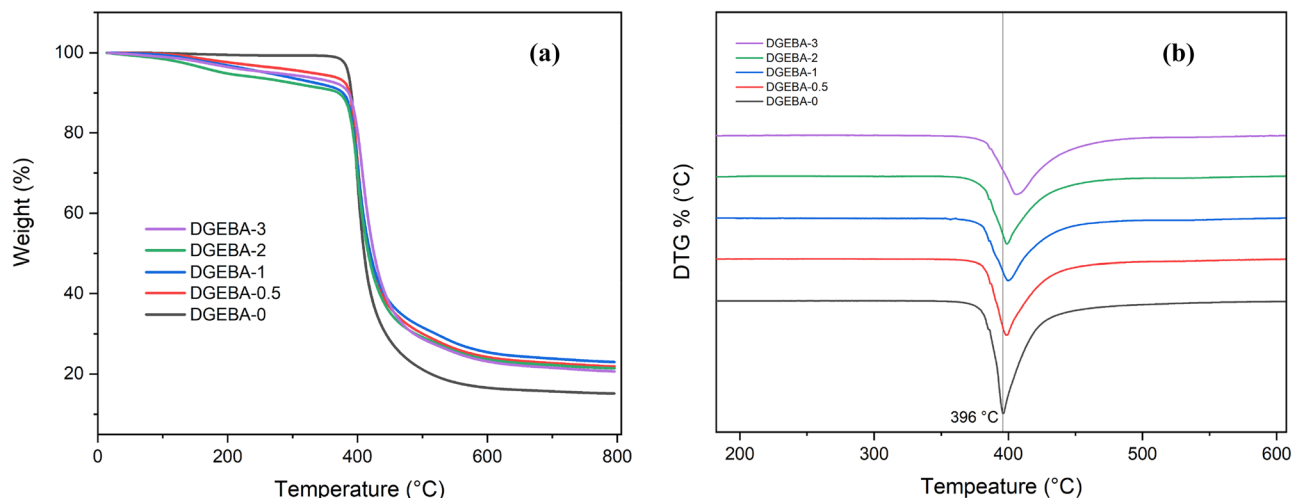


Fig. 8 DSC curves for DGEBA and its blends



**Fig. 9** **a** comparison of TGA curves of neat DGEBA with its blends and **b** First derivative of weight loss percentage against temperature curve (DTG) indicates the increase in degradation temperature with the increased addition of BPC complex

as shown in Fig. 9b. High char yield may have influenced lower flammability as confirmed in the vertical burning test. Increased char formation can limit the production of combustible carbon-containing gases, decrease the exothermicity due to pyrolysis reactions, and decrease the thermal conductivity of the surface of a burning material [47].

Data in Table 2 illustrate percentage weight loss at some important temperature points. It leads to an interesting fact that at 100 °C, the percentage weight loss of all blends and neat DGEBA are relatively equivalent. The decomposition temperature of neat DGEBA was higher than that of blends up to 390 °C. But from 400 °C onwards, the decomposition temperature of blends increased with minimised polymer mass loss. Percentage weight of DGEBA-0 (6%) was lower than DGEBA-0.5 (7%) and DGEBA-1 (7%) meaning the blend has better weight stability compared to the neat DGEBA above 400 °C. Neat epoxy lost 31.95% of its original weight at 400 °C due to the presence of volatile components. Slower degradation of blends over 400 °C is attributed to the formation of dense and stable char layer that protected the underlying epoxy resin from further

degradation. Increased addition of BPC complex in polymer promoted degradation of epoxide in the 100 to 400 °C region promoting early formation of thick stable layer of char that enhanced the thermal stability over 400 °C by participating in charring. This is further confirmed by the images from optical microscope (Fig. 16). The amount of char formed at 800 °C indicated the presence of non-combustible inorganic boron compound in the blend [48]. Neat DGEBA left a residue of 5% whereas DGEBA-0.5 and DGEBA-1 produced over 0% char residue. TGA graphs of neat DGEBA and its blends are shown in Fig. 9a.

A useful result obtained from TGA analysis is the statistic heat resistance index (*T<sub>s</sub>*) and is calculated with the temperature of degradation at 5% and 30% using Eq. (1). *T<sub>s</sub>* of neat DGEBA is 193 °C and *T<sub>s</sub>* decreased gradually with increased amount of additive up to 40 phr and then increased as shown in Table 3. Decrease in *T<sub>s</sub>* of blends compared to neat DGEBA is attributed to lower thermal stability of the blend under 400 °C which is re-confirmed by TGA data analysis [7].

$$T_s = 0.49[T_{-5\%} + 0.6(T_{-30\%} - T_{-5\%})] \tag{1}$$

**Table 2** Percentage mass of neat DGEBA and blends at various temperatures

Blend	% Wt. at 100 °C	% Wt. at 390 °C	% Wt. at 400 °C	% Wt. at 410 °C	% Wt. at 420 °C	% Wt. at 430 °C	% Wt. at 475 °C	Char @ 795 °C
DGEBA-0	99.9	91.7	68.1	50.3	40.3	34.7	24.0	15.2
DGEBA-0.5	99.7	88.0	73.0	58.3	49.0	43.0	33.6	22.0
DGEBA-1	99.4	84.4	72.0	58.5	50.0	44.1	34.0	23.0
DGEBA-2	99.9	83.1	70.0	56.0	47.4	41.7	31.4	21.4
DGEBA-3	99.0	88.5	80.4	66.6	55.0	47.0	33.0	21.0
DGEBA-5	99.6	84.4	75.0	61.5	51.0	43.0	29.0	19.3

**Table 3** tatic heat resistance index (Ts) of neat DGEBA and blends

Blend	Temp at T-5%	Temp at T-30%	Ts (°C)
DGEBA-0	386	399	193
DGEBA-0.5	329	402	183
DGEBA-1	261	401	169
DGEBA-2	194	400	156
DGEBA-3	271	408	173
DGEBA-5	305	404	179

### Flammability tests

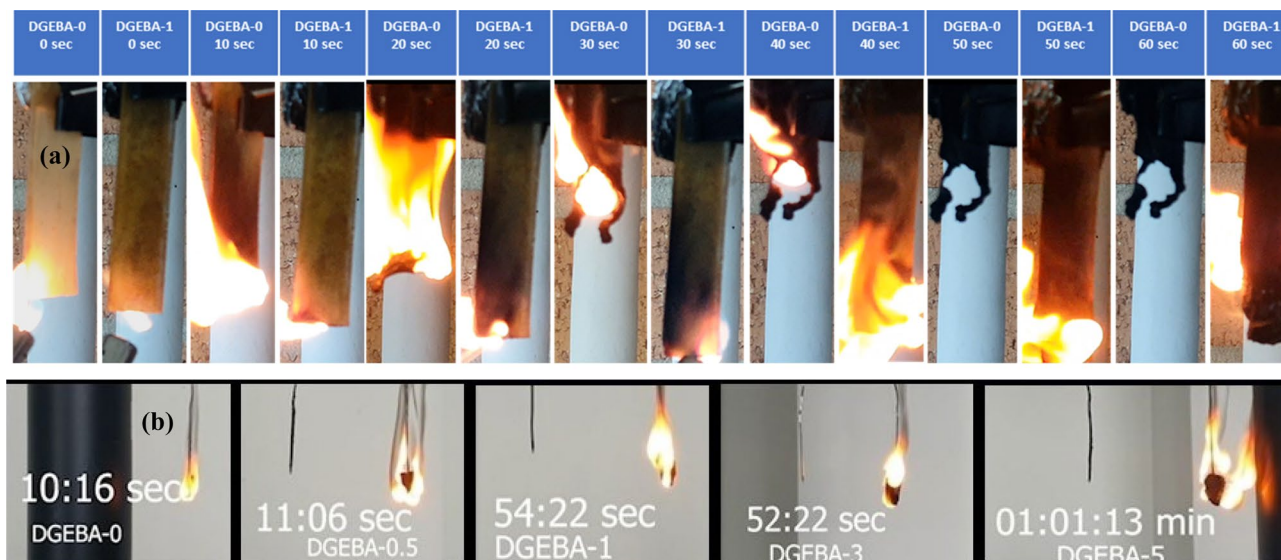
Vertical burning test of samples revealed that the epoxy blends with BPC fire retardant showed improved flame retardancy with self-extinguishing properties compared to the neat epoxy. A comparison of flammability test between neat epoxy and DGEBA-1 in 10 s interval is shown in Fig. 10a. DGEBA-1 was chosen for comparison due to the deterioration of mechanical properties in the higher blend compositions. Both samples were ignited within 10 s of exposure to flame. Neat DGEBA was completely burned within 50 s. DGEBA-1 self-extinguished within 15 s. A blowing out effect of DGEBA-1 is obvious to cause quenching at 20 s. Second ignition self-extinguished in 55 s. Third and fourth ignition self-extinguished quickly within 10 and 20 s. DGEBA was introduced to flame after every self-ignition to test its ability to retard fire after initial ignition. The total burning event lasted for 80 s and retained its shape and size after complete ignition as seen at 60 s. A polymer with high aromatic ring content in the chain backbone usually has high heat and flame resistance [47].

**Table 4** Vertical burning test ratings of neat and blend epoxy resins

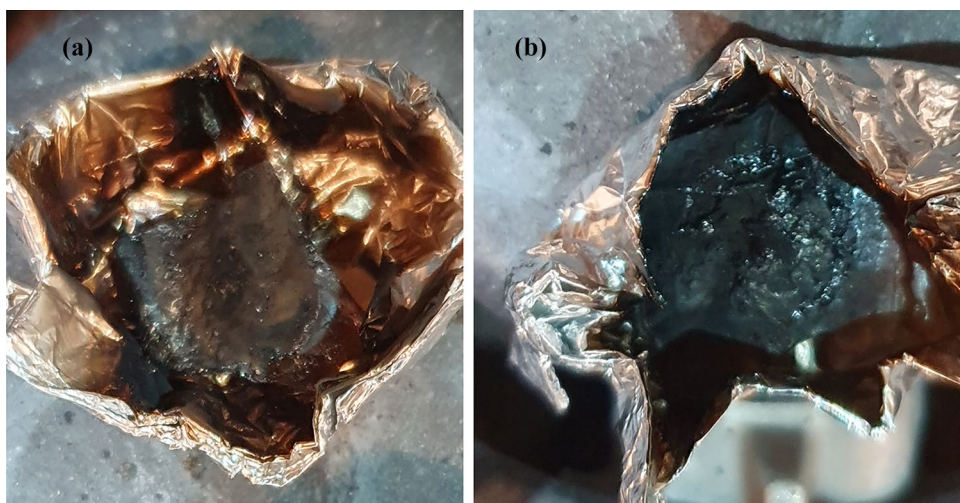
Sample	UL-94
DGEBA-0	NR
DGEBA-1	V-1
DGEBA-2	V-0
DGEBA-3	V-0
DGEBA-5	V-0

A complete combustion was observed for DGEBA-0.5, but DGEBA-3 self-extinguished in 2 s. DGEBA-5 self-extinguished in multiple occasions within first 50 s and failed to ignite from normal flame after the char formation. High temperature torch was utilised to ignite thereafter. Blends from DGEBA-1 onwards demonstrated better fire retardancy and self-extinguishing properties. The improved UL-94 rating of the epoxy blend is attributed to the presence of boron compound in the epoxy matrix [49]. The vertical burning test ratings for the neat epoxy and the blends are shown in Table 4.

Random shaped blends were ignited to identify the combustion time as shown in Fig. 10b. The results prove self-extinguishing properties and non-flammability with the increased addition of BPC fire retardant to the polymer matrix. The neat epoxy and DGEBA-1 were exposed to fire in an aluminium foil to observe the char formation. It was identified that neat epoxy undergone complete combustion and DGEBA-1 formed a layer of char on the surface of the specimen as shown in Fig. 11. The vertical burning photographs of DGEBA-1 at 25 and 80 s were shown in Fig. 12.

**Fig. 10** a Flammability of neat DGEBA and 20phr blend, b Flammability of neat DGEBA and blends in randomly shaped samples

**Fig. 11** **a** Complete combustion of neat epoxy and **b** char formation on DGEBA-1 surface



**Cone calorimetry**

Three sets of carbon fibre reinforced epoxy composites were prepared by hand layup method using room temperature curing resin, kinetix R118 and H120 hardener. Three layers of carbon

fibre woven sheets were used for each set. Each layer was wetted out with resin by hand using a brush. The first set was wetted out with neat epoxy (CFR-EP), the second set was wetted out with 8 wt% BPC epoxy blend (CFR-FREP-1) and the third set was wetted out with 16 wt% BPC-epoxy blend (CFR-FREP-2). Every layer in each set was separately coated, and a final coat of epoxy was applied on the surface of the third layer. The mixing ratio and other details of the carbon fibre reinforced composites are described in Table 5 and an illustration is presented in Fig. 13. The composites were cured at room temperature for 24 h and tested for reaction to fire performance under a cone calorimeter.

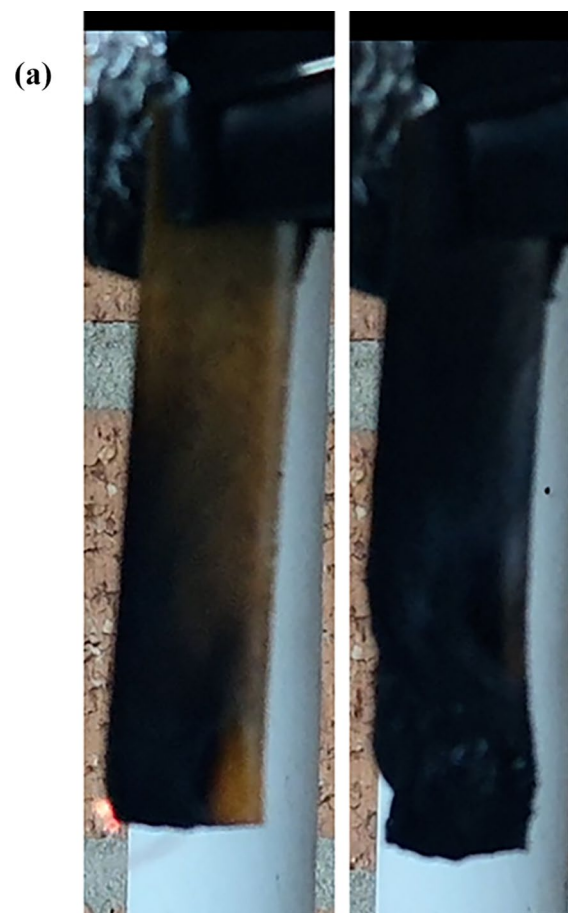


**Fig. 12** Vertical burning event photos of DGEBA-1 at **a** 25 s and **b** 80 s to compare the surface char formation

As described in Table 6, the time to ignition of the FREP composites were shorter than the neat EP. This is caused by the weakened resistance to ignition by the presence of BPC. This result is similar to the findings from TGA analysis where early decomposition of EP-BPC blends were detected as described in Table 2 [50]. The peak heat release rate (peak HRR) of the modified epoxy system was reduced with increased addition of BPC complex. The neat EP composite burned rapidly with the peak HRR of 1234.4 kW/m<sup>2</sup> but the addition of 8 wt% of BPC to the EP composite system reduced the peak HRR to 1129 kW/m<sup>2</sup> and 16 wt% of BPC decreased the Peak HRR to 876.4 kW/m<sup>2</sup>. Moreover, the total smoke release (TSR) was decreased with increased addition of BPC

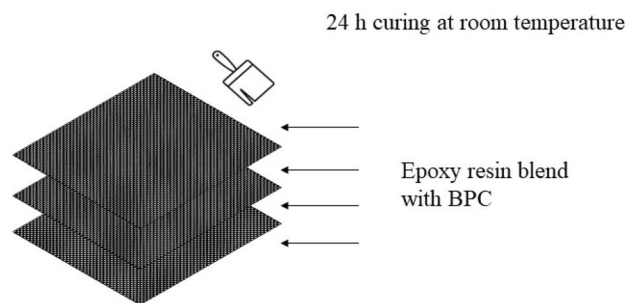


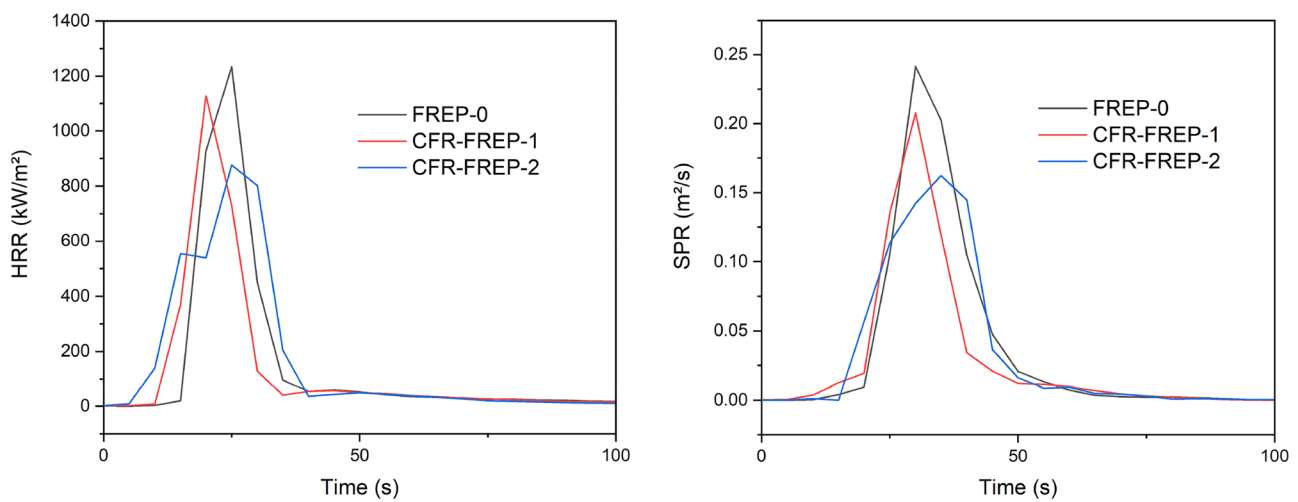
**Fig. 13** Preparation of carbon fibre reinforced epoxy composite.

**Table 5** Mixing ratio of carbon fibre reinforced epoxy polymers

Samples	R118 resin (g)	H120 hardener (g)	BPC (g)	Number of CF layers	Final wt. (g)
CFR-EP	24	6	0	3	11.41
CFR-FREP-1	24	6	2	3	11.44
CFR-FREP-2	24	6	4	3	11.42

**Table 6** Cone calorimetry test results of neat and fire-retardant carbon fibre reinforced composite

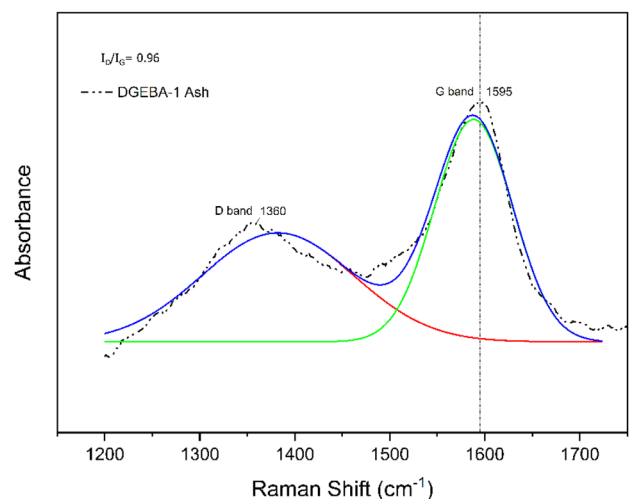
Samples	TTI (s)	Peak HRR (kW/m <sup>2</sup> )	THR (MJ/m <sup>2</sup> )	TSR (m <sup>2</sup> /m <sup>2</sup> )	TSP (m <sup>2</sup> )
CFR-EP	21	1234.4	14.95	436.0	3.9
CFR-FREP-1	16	1129.0	17.99	341.2	3.6
CFR-FREP-2	11	876.4	14.19	404.0	3.0

**Fig. 14** Heat release rate and smoke production rate of carbon fibre composites of neat epoxy, 8 wt % FR and 16 Wt% FR composite

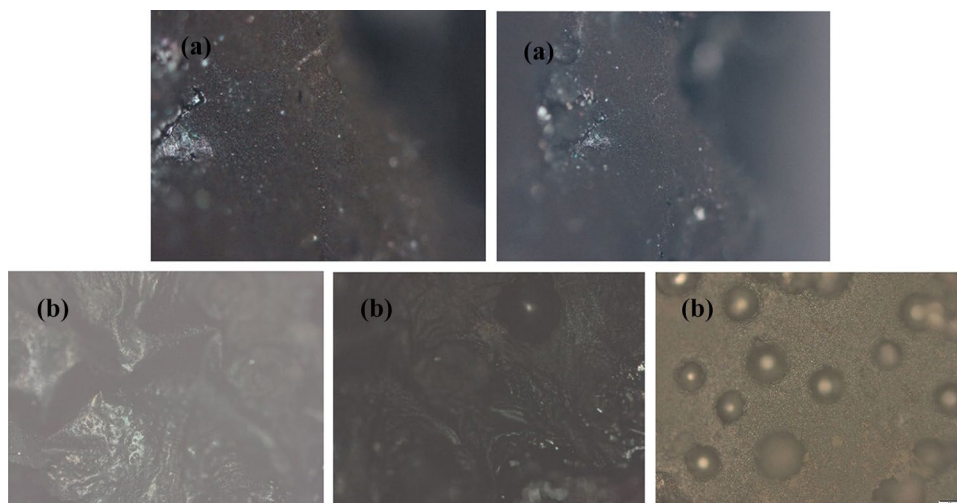
in the composite. The neat EP composite released 436 m<sup>2</sup>/m<sup>2</sup> smoke, whilst the 8 wt% and 16 wt% BPC composites showed significant reduction in total smoke production with 341.2 m<sup>2</sup>/m<sup>2</sup> and 404.0 m<sup>2</sup>/m<sup>2</sup> respectively. A gradual minor decrease in the total smoke production (TSP) was observed in the FREP composites compared to the neat EP composite. The reduced smoke production is attributed to the presence of boron compound in the epoxy matrix [51]. The boron containing BPC was bonded to the epoxy matrix to prevent further ignition. The bonding was confirmed with FTIR analysis and char formation was confirmed with Raman spectroscopy. The heat release rate and smoke production rate of the composites are shown in Fig. 14.

### Raman spectroscopy

Raman spectroscopy is generally adopted to investigate the order degree of carbonaceous materials. Raman spectrum of burned and unburned DGEBA-1 was captured using a 514 nm edge laser beam. There were two distinctive peaks

**Fig. 15** Raman spectrum of DGEBA-1 showing significant D and G band peaks

**Fig. 16** Optical microscope images of **a** burned surface of neat DGEBA and **b** DGEBA-1 showing thick layer of char



at  $1360\text{ cm}^{-1}$  and  $1595\text{ cm}^{-1}$  from char section that linked to D and G bands as shown in (Fig. 15). The unburned DGEBA-1 did not have a peak. The D and G bands were attributed to the breathing and scattering of phonon [52, 53]. D band corresponds to breathing mode of k-point phonons  $A_{1g}$  symmetry and G band is the first order scattering of  $E_{2g}$  phonons [54]. Degree of graphitization is calculated from the ratio of integrated intensities of D and G band (ID/IG). The ratio of the relative peak intensity of the D band and G band is a measure of disorder degree and average size of the  $sp^2$  domains in graphite materials [55]. A lower ID/IG value indicated higher degree of graphitization. The ID/IG value of DGEBA-1 exhibited a lower value of 0.96 from Raman spectral data whereas neat DGEBA value was higher (4.2, according to the literature) [56, 57]. This indicated higher degree of graphitization for DGEBA-1. This was attributed to the early thermal degradation and char formation on the epoxy surface due to the enhanced thermal conductivity. More char was formed with graphitisation structure triggered by boron compounds.

### Optical microscope

Figure 16a, b were the optical microscope images of char layer from the neat DGEBA and DGEBA-1. The surface of the char layer was unstable and uneven and porous for neat DGEBA, whereas images of DGEBA-1 confirmed nonporous, continuous thick layer of char.

### Conclusion

An intrinsically modified fire retardant epoxy system was synthesized using boron polyol complex (BPC), blended with DGEBA epoxy resin. Intermolecular hydrogen bonding between BPC complex and DGEBA was confirmed by

FTIR spectrum analysis. The thermal conductivity of the epoxy resin was improved by enhanced phonon transport through hydrogen bonding. D and G bands of Raman spectrum confirmed breathing and scattering of phonons in the char of the epoxy BPC blend with high degree of graphitization. Thermogravimetric analysis results confirmed an increase of over 20% char formation in condensed phase. Formation of char in early stage of combustion below  $400\text{ }^\circ\text{C}$  was confirmed by 5 wt% decomposition temperature data analysis. Improved thermal stability of the blend was attributed to the higher char yield and presence of non-combustible inorganic boron compounds. The char protected underlying DGEBA epoxy from further burning. Improved thermal conductivity and presence of boron in DGEBA promoted early thermal degradation and char formation. A blowing out effect and self-extinguishing property during ignition was caused by the formation and quick emission of pyrolytic gases in condensed phase. This was also attributed to the thick layer of char beneath which the gases accumulate and was verified by optical microscope images. Cone calorimetry testing proved reduced peak heat release rate and smoke production with the increased addition of BPC complex. The UL-94 vertical burning tests confirmed that a 20 phr blend of BPC with the epoxy achieve V-1 rating and 40 phr blend achieve V-0 rating. Ultimately, the fire-retardant thermoset preserved its size and shape after 80 s of complete combustion that involved multiple self-extinguishing events.

**Supplementary Information** The online version contains supplementary material available at <https://doi.org/10.1007/s10965-023-03641-6>.

**Funding** Open Access funding enabled and organized by CAUL and its Member Institutions The authors acknowledge the Faculty of Science, Engineering and Technology (FSET) of Swinburne University of Technology Melbourne for the financial support provided to the first author, having been awarded a masters by research studentship;

and research grants from the Australian Research Council for the ARC DECRA (DE170101249) and Linkage Projects (LP200301659).

**Data availability** The authors declare that the data supporting the findings of this study are available within the paper and its Supplementary Information files. Should any raw data files be needed in another format they are available from the corresponding author upon reasonable request.

## Declarations

**Conflicts of interest** There are no Conflicts of interests/Competing interests to declare.

**Open Access** This article is licensed under a Creative Commons Attribution 4.0 International License, which permits use, sharing, adaptation, distribution and reproduction in any medium or format, as long as you give appropriate credit to the original author(s) and the source, provide a link to the Creative Commons licence, and indicate if changes were made. The images or other third party material in this article are included in the article's Creative Commons licence, unless indicated otherwise in a credit line to the material. If material is not included in the article's Creative Commons licence and your intended use is not permitted by statutory regulation or exceeds the permitted use, you will need to obtain permission directly from the copyright holder. To view a copy of this licence, visit <http://creativecommons.org/licenses/by/4.0/>.

## References

- Capricho JC, Fox B, Hameed N (2020) Multifunctionality in Epoxy Resins. *Polym Rev* 60(1):1–41
- Chen L et al (2019) Intrinsic flame-retardant epoxy resin composites with benzoxazine: Effect of a catalyst and a low curing temperature. *J Appl Polym Sci* 136(33):47847–n/a
- Huang S et al (2021) Novel Ti<sub>3</sub>C<sub>2</sub>T<sub>x</sub> MXene/epoxy intumescent fire-retardant coatings for ancient wooden architectures. *J Appl Polym Sci* 138(27):n/a
- Ai Y-F et al (2020) Multifunctional phosphorus-containing Triazolyl Amine toward Self-Intumescent Flame-Retardant and mechanically strong Epoxy Resin with high transparency. *Ind Eng Chem Res* 59(26):11918–11929
- Feng Y et al (2020) Multiple synergistic effects of graphene-based hybrid and hexagonal born nitride in enhancing thermal conductivity and flame retardancy of epoxy. *Chem Eng J* 379
- Li Z et al (2018) Covalent assembly of MCM-41 nanospheres on graphene oxide for improving fire retardancy and mechanical property of epoxy resin. *Compos Part B: Eng* 138:101–112
- Niu H et al (2021) Phosphorus-free vanillin-derived intrinsically flame-retardant epoxy thermoset with extremely low heat release rate and smoke emission. *ACS Sustain Chem Eng* 9(15):5268–5277
- Dai J et al (2019) Synthesis of bio-based fire-resistant epoxy without addition of flame retardant elements. *Compos Part B Eng* 179:107523
- Tian Y et al (2020) A renewable resveratrol-based epoxy resin with high tg, excellent mechanical properties and low flammability. *Chem Eng J* 383:123124
- Favstritsky N, Wang J (1997) Flame-retardant brominated styrene-based polymers. X. Dibromostyrene grafted latexes. *J Coatings Technol* 69(868):39–44
- Blum A et al (2019) Organophosphate ester flame retardants: are they a regrettable substitution for polybrominated diphenyl ethers? *Environ Sci Technol Lett* 6(11):638–649
- Schartel B et al (2007) Pyrolysis of epoxy resins and fire behavior of epoxy resin composites flame-retarded with 9,10-dihydro-9-oxa-10-phosphaphenanthrene-10-oxide additives. *J Appl Polym Sci* 104(4):2260–2269
- Wath SB et al (2015) Separation of WPCBs by dissolution of brominated epoxy resins using DMSO and NMP: a comparative study. *Chem Eng J* 280:391–398
- Lloyd J (1997) International status of borate preservative systems. In: *Proceedings of the Second International Conference on Wood Protection with Diffusible Preservatives and Pesticides*
- LeVan SL, Tran HC The role of boron in flame-retardant treatments
- Capricho J et al (2017) Incorporation of boron complex into resin. Google Patents
- Winandy J (1997) Effects of fire retardant retention, borate buffers, and redrying temperature after treatment on thermal-induced degradation. *For Prod J* 47(6):79–86
- Shen KK (2014) Chap. 11 - Review of Recent Advances on the Use of Boron-based Flame Retardants. In: *Papaspyrides CD, Kiliaris P (Eds), Polymer green flame retardants*. Elsevier: Amsterdam. p 367–388
- Chen S et al (2020) Synthesis and application of a triazine derivative containing boron as flame retardant in epoxy resins. *Arab J Chem* 13(1):2982–2994
- Yang S, Zhang Q, Hu Y (2016) Synthesis of a novel flame retardant containing phosphorus, nitrogen and boron and its application in flame-retardant epoxy resin. *Polym Degrad Stab* 133:358–366
- Zeng Y et al (2019) Exposure of hydrocarbon intumescent coatings to the UL1709 heating curve and furnace rheology: effects of zinc borate on char properties. *Prog Org Coat* 135:321–330
- Touval I (1993) Antimony and other inorganic flame retardants. In: *Krik-Othmer (ed) Encyclopaedia of Chemical Technology*, p 936–954
- Ullah S et al (2017) Effects of ammonium polyphosphate and boric acid on the thermal degradation of an intumescent fire retardant coating. *Prog Org Coat* 109:70–82
- Chen J et al (2015) Preparation and characterization of graphene oxide reinforced PVA film with boric acid as crosslinker. *J Appl Polym Sci* 132(22):n/a–n/a
- Demirel M, Pamuk V, Dilsiz N (2010) Investigation of flame retardancy and physical–mechanical properties of zinc borate/boric acid polyester composites. *J Appl Polym Sci* 115(5):2550–2555
- Mukhopadhyay C, Datta A, Butcher RJ (2009) Highly efficient one-pot, three-component Mannich reaction catalysed by boric acid and glycerol in water with major ‘syn’ diastereoselectivity. *Tetrahedron Lett* 50(29):4246–4250
- Halimehjani AZ, Gholami H, Saidi MR (2012) Boric acid/glycerol as an efficient catalyst for regioselective epoxide ring opening by aromatic amines in water. *Green Chem Lett Rev* 5(1):1–5
- Mehra N, Li Y, Zhu J (2018) Small Organic Linkers with Hybrid terminal groups drive efficient Phonon Transport in Polymers. *J Phys Chem C* 122(19):10327–10333
- Kim G-H et al (2015) High thermal conductivity in amorphous polymer blends by engineered interchain interactions. *Nat Mater* 14(3):295–300
- Vlasov A, Florinskaya V, Venediktov A (1974) Structure and Physicochemical Properties of Inorganic Glasses. *Khimiya, Leningrad*, pp 285–350
- Medvedev EF, Komarevskaya AS (2007) IR spectroscopic study of the phase composition of boric acid as a component of glass batch. *Glass Ceram* 64(1):42–46
- Zheng G et al (2011) The synthesis of high yield diglycerin borate. *Appl Mech Mater* 55–57:312–316

33. Hameed N et al (2010) Reactive block copolymer modified thermosets: highly ordered nanostructures and improved properties. *Soft Matter* 6(24):6119–6129
34. Wu S et al (2012) A new route to nanostructured thermosets with block ionomer complexes. *Soft Matter* 8(3):688–698
35. Hameed N et al (2015) Ductile thermoset polymers via controlling network flexibility. *Chem Commun* 51(48):9903–9906
36. Carrell HL, Whalen DL, Glusker JP (1997) Hydrogen bonding incis-2,3-epoxycyclooctanol. *Struct Chem* 8(2):149–154
37. June Sutor D (1962) The C–H... o hydrogen bond in crystals. *Nature* 195(4836):68–69
38. Nakamura S, Tsuji Y, Yoshizawa K (2020) Role of Hydrogen-Bonding and OH –  $\pi$  interactions in the adhesion of Epoxy Resin on Hydrophilic Surfaces. *ACS Omega* 5(40):26211–26219
39. Salim NV et al (2015) Novel Approach to trigger nanostructures in Thermosets using Competitive Hydrogen-Bonding-Induced phase separation (CHIPS). *Macromolecules* 48(22):8337–8345
40. Salehpour S, Dubé MA (2012) Reaction monitoring of glycerol step-growth polymerization using ATR-FTIR spectroscopy. *Macromol React Eng* 6(2–3):85–92
41. White RP, Lipson JEG (2016) Polymer free volume and its connection to the Glass Transition. *Macromolecules* 49(11):3987–4007
42. Zang L et al (2011) Novel Star-shaped and hyperbranched phosphorus-containing flame retardants in Epoxy Resins. *Polym Adv Technol* 22(7):1182
43. Liu J-K et al (2011) Tailored thermal and mechanical properties of epoxy resins prepared using multiply hydrogen-bonding reactive modifiers. *J Appl Polym Sci* 120(4):2411–2420
44. Tang H, Zhou H (2020) A novel nitrogen, phosphorus, and boron ionic pair compound toward fire safety and mechanical enhancement effect for epoxy resin. *Polym Adv Technol* 31(4):885–897
45. Yang S et al (2016) Synergistic flame-retardant effect of expandable graphite and phosphorus-containing compounds for epoxy resin: strong bonding of different carbon residues. *Polym Degrad Stab* 128:89–98
46. Wu H et al (2019) An intramolecular hybrid of metal polyhedral oligomeric silsesquioxanes with special titanium-embedded cage structure and flame retardant functionality. *Chem Eng J* 374:1304–1316
47. Lin SC, Pearce EM (1979) Epoxy resins. II. The preparation, characterization, and curing of epoxy resins and their copolymers. *J Polym Science: Polym Chem Ed* 17(10):3095–3119
48. Dogan M, Murat S, Unlu (2014) Flame retardant effect of boron compounds on red phosphorus containing epoxy resins. *Polym Degrad Stab* 99:12–17
49. Tang S et al (2018) Synergistic flame-retardant effect and mechanisms of boron/phosphorus compounds on epoxy resins. *Polym Adv Technol* 29(1):641–648
50. Li X et al (2018) Highly thermally conductive flame retardant epoxy nanocomposites with multifunctional ionic liquid flame retardant-functionalized boron nitride nanosheets. *J Mater Chem Mater energy Sustain* 6(41):20500–20512
51. Xu Z, Chu Z, Yan L (2018) Enhancing the flame-retardant and smoke suppression properties of transparent intumescent fire-retardant coatings by introducing boric acid as synergistic agent. *J Therm Anal Calorim* 133:1241–1252
52. Liu J et al (2013) The dependence of Graphene Raman D-band on Carrier Density. *Nano Lett* 13(12):6170–6175
53. Matthews MJ et al (1999) Origin of dispersive effects of the Raman D band in carbon materials. *Phys Rev B* 59(10):R6585
54. Yu B et al (2015) Enhanced thermal and flame retardant properties of flame-retardant-wrapped graphene/epoxy resin nanocomposites. *J Mater Chem Mater energy Sustain* 3(15):834–844
55. Niyogi S et al (2010) Spectroscopy of covalently functionalized graphene. *Nano Lett* 10(10):4061–4066
56. Zhu Z et al (2020) A facile one-step synthesis of highly efficient melamine salt reactive flame retardant for epoxy resin. *J Mater Sci* 55(27):12836–12847
57. Zhang Z et al (2019) Synthesis of CeO<sub>2</sub>-loaded titania nanotubes and its effect on the flame retardant property of epoxy resin. *Polym Adv Technol* 30(8):2136–2142

**Publisher's Note** Springer Nature remains neutral with regard to jurisdictional claims in published maps and institutional affiliations.